CONTROLS ON BIOGENIC METHANE FORMATION IN CHEROKEE BASIN COALBEDS, KANSAS

by

BRIEN WILSON

B.S., University of Oklahoma 2013

A THESIS

submitted in partial fulfillment of the requirements for the degree

MASTER OF SCIENCE

Department of Geology
College of Arts and Sciences

KANSAS STATE UNIVERSITY
Manhattan, Kansas

2015

Approved by:

Major Professor
Dr. Matt Kirk

Copyright

Abstract

The Cherokee basin in southeastern Kansas is a declining coalbed methane (CBM) field where little is known about how the CBM formed, the extent to which it continues to form, and what factors influence its formation. An understanding of methanogenic processes and geochemistry could lead to potential enhancement of methane formation in the basin. The objectives of this project are to (1) determine the pathway of methane formation and (2) determine whether geochemistry has influenced gas formation. In order to reach the objectives, we analyzed formation water geochemistry, production history, and gas composition and isotopes. Post Rock Energy Corporation gave us access to 16 wells for sampling purposes. We collected gas samples in Isotubes® for compositional and isotopic analyses at a commercial laboratory. We analyzed major ion chemistry from formation water using standard methods. Co-produced water samples we collected are Na-Cl type with total dissolved solids content ranging from 35,367 to 91,565 mg/L. TDS tended to be highest in samples collected from wells with greater total depth. The pH and temperature of sampled water averaged 7.0 and 19°C with an alkalinity ranging from 3.33 to 8.59. Gas dryness and $\delta^{13}C$ CH_4 range from 196 to 4531 and -69.95 to -56.5, respectively, which indicate that methane is being produced biologically. Comparing the $\delta^{13}C$ CH_4 to the δD CH_4, which ranges from -228.2 to -217.2, suggest that the primary pathway of methanogenesis is H_2/CO_2 reduction. We calculated Δ (the difference between δ values) in order to correlate isotope data to produced water chemistry. Samples ΔD and $\Delta^{13}C$ values range from -189.1 to -168.7 and 61.52 to 69.99. Calculated $\Delta D_{CH4\text{-}H2O}$ and $\Delta^{13}C_{CO2\text{-}CH4}$ values approach the range for the acetate/methyl pathways as Cl^- concentration increases, potentially indicating a slight shift in methanogenic pathway in deeper, more saline

portions of the basin. The culturing results revealed that living methanogens are still able to utilize H_2, acetate, and methanol present in co-produced formation water from all tested wells.

Table of Contents

List of Figures

List of Tables

Acknowledgements

I would like to thank my advisor Dr. Matt Kirk for all of his help and wise words. Without his inspiration and guidance this project would never have been completed. All of the weekly meetings, e-mails, and long hours spent editing my writings were greatly appreciated. I will carry his advice with me into my life and future career.

I would also like to thank my committee members Dr. Allen Archer and Dr. Saugata Datta. Their advice and assistance with this project were extremely helpful.

Last but not least I would like to thank my family and friends. Without their support I would not have made it this far. I would especially like to thank my fiancé Brianna Kwasny. Her support throughout graduate school has been vital in the realization of my master's thesis.

Chapter 1 - Introduction

Natural gas is very important for the United States' future energy program. Using natural gas as a fuel source has the potential to lead to lower greenhouse gas emissions. Combustion of natural gas produces half the CO_2 of coal per energy generated. The domestic quantity of producible natural gas is growing. Production technology and drilling advancements have allowed reserves in the United States to increase from 322.7 to 354 tcf (trillion cubic feet) (U.S. Energy Information Administration, 2014).

Natural gas can form in the subsurface from two different processes: (1) thermocatalytic reactions and (2) microbiological reactions. Natural gas forms via thermocatalytic reactions when organic matter is buried deep in the subsurface and heated (Fig. 1). The second process is from microbial degradation (biogenic) of organic matter. Biogenic gas formation requires a consortium of microorganisms. Bacteria degrade complex organic matter and produce simple substrates that methanogenic archaea use to make natural gas. Substrates used by archaea fall into three categories: H_2/CO_2 reduction, acetate fermentation, and from methylated compounds (Table 1).

Table 1. Chemical reactions representing the three biogenic methane pathways.

H_2/CO_2 Reduction
$H_2 + ¼\ CO_2 \rightarrow ¼\ CH_4 + ½\ H_2O$
Acetate Fermentation
$CH_3COO^- + H^+ \rightarrow CO_2 + 2\ H_2O$
Methylated Compounds
$4\ CH_3OH \rightarrow 3\ CH_4 + CO_2 + 2\ H_2O$

Understanding the controls on biogenic gas formation could offer opportunities to increase commercial gas production and limit environmental impacts. Many natural gas reservoirs could presently have biologic reactions occurring. If the microorganisms are still there, then the addition of food could enhance their production of methane. By using produced water to re-supply the microbes with food, we could cut down on disposal amounts. Enhancing methane formation and subsequent production would decrease the amount of wells necessary to make a field economic. Drilling fewer wells would also decrease the amount of produced water to dispose.

In this study, we aim to determine if biological processes produce methane in the Cherokee basin (CHB), and if so, what controls methane formation. The CHB is a promising field location for geomicrobiological research for multiple reasons. The Cherokee group coals are buried relatively shallow (~400' - 1200') and show immature to mature R_o values (0.5% to 0.7%), suggesting that thermogenic gas is unlikely to be the sole source of methane formation (Newell, 2012). Maximum burial depth is calculated to be ~6,000 feet deep by Pennsylvanian and Permian sediments (Barker et al., 1992). Type I and II organic matter buried that deep would just reach the oil generation window and definitely not reach dry gas generation (Fig. 1). The field averaged 20 Mcfd/well with a cumulative production of 165 bcf as of 2008 (Newell, 2010). Because the R_o values are too low for gas generation, it is unlikely that thermal maturity alone could account for that quantity of gas (Newell, 2010). Finally, the CHB is a good location for this research because the field is in decline. By studying gas formation, we may be able to develop strategies to increase the life of the basin's CBM wells.

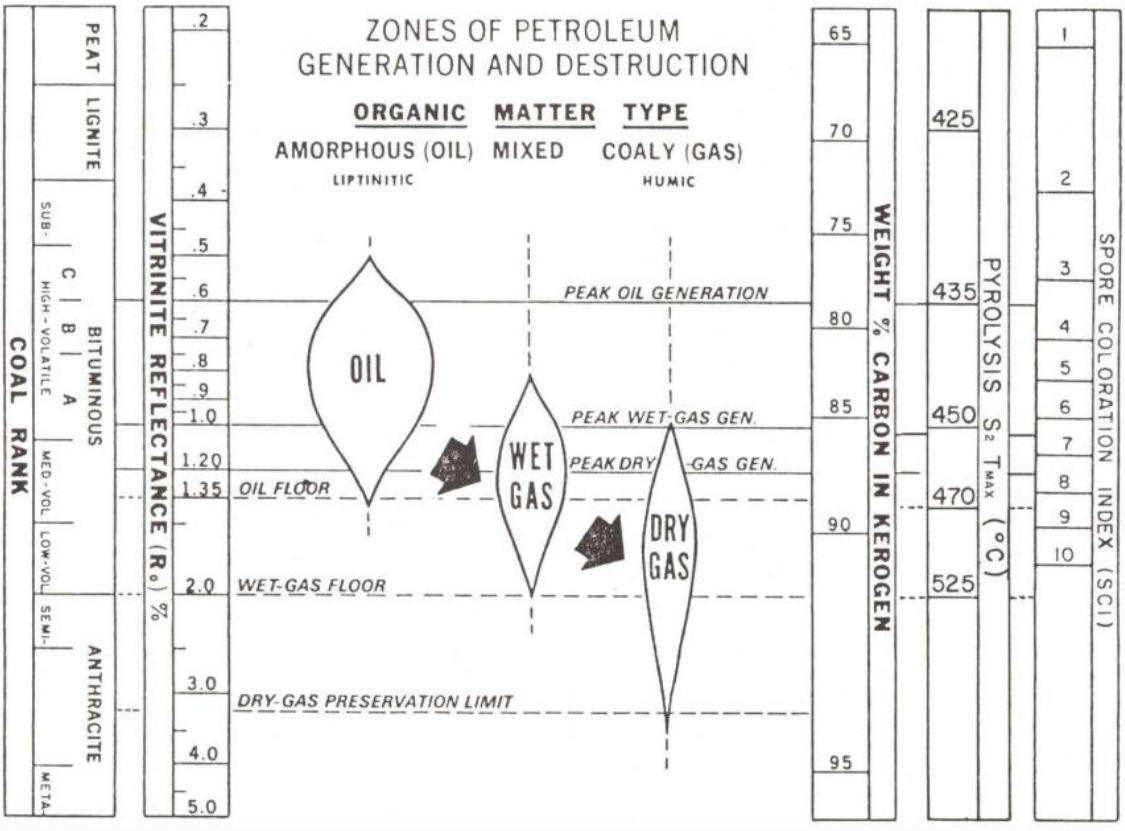

Figure 1. Oil, wet gas, and dry gas generation windows relative to coal rank, vitrinite reflectance, weight % carbon in kerogen, pyrolysis, and SCI (Dow & O'Connor, 1982).

Chapter 2 - Hypotheses

The research objective of this study is to test the following hypotheses: (1) a portion of the natural gas in Cherokee Basin coalbeds was formed biologically and (2) that formation water geochemistry influenced natural gas formation. In order to test these hypotheses, we performed a field study that integrated formation water geochemistry, gas composition, production data, and lab experiments. Specific questions that we aimed to answer are as follows:

1. How did gas in the coalbeds form?
2. Are living cells capable of forming methane present in the coalbeds?
3. How does formation water geochemistry vary across the basin?
4. Are there relationships between water chemistry and gas composition with production?

Chapter 3 - Geologic Setting

3.1 Eastern Kansas Structural Geometry

There are five structural features that are important in describing the subsurface in Eastern Kansas. The Forest City basin is located in the northeast corner of Kansas and is separated from the CHB to the south by the Bourbon arch. Both basins are bound to the west by the Nemaha ridge that starts at the border of Oklahoma and continues north into Nebraska (Lange, 2003) (Fig. 2). The Ozark dome in southwestern Missouri creates the eastern flank of the CHB. To the south, the CHB deepens into the Arkoma basin of Oklahoma and Arkansas.

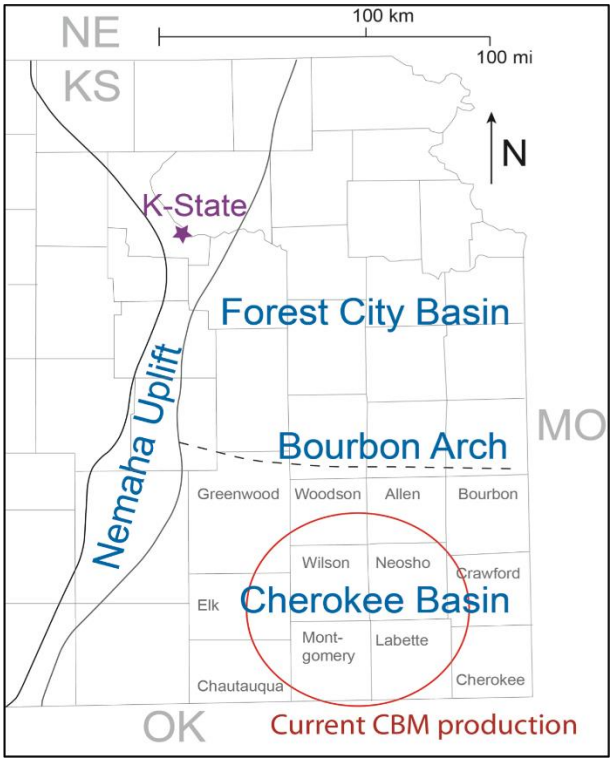

Figure 2. Map of eastern Kansas showing regional structural features. Red circle is around field study location which coincides with the primary location of current CBM production in the CHB.

During Cherokee deposition, eastern Kansas was located on a shelf that represented the northern extension of the foreland Arkoma basin in eastern Oklahoma and western Arkansas.

The Arkoma basin was formed due to continental collision and the subsequent Ouachita Orogeny (Sutherland, 1988). By the end of the Mississippian, the Ozark dome in western Missouri had been completely developed (Merriam, 1962), which created a slight 0.5º dip to the west until the Cherokee Group reaches the Humboldt fault zone and associated Nemaha ridge (Fig. 2) (Lange, 2003). The Nemaha Ridge was formed pre-Pennsylvanian due to normal faulting in the Humboldt fault zone (Walton, 1996).

3.2 Cherokee Group Stratigraphy

Natural gas wells sampled in this study are completed in the Cherokee Group of Pennsylvanian age. Pennsylvanian rocks in Kansas are predominantly limestones, but the Cherokee Group in the CHB consists of sandstones, shales, and coals (Woody, 1982-1985). Pennsylvanian rocks in this area lay disconformably on Mississippian limestones due to karst topography at the end of Mississippian times (Lange, 2003). Cherokee group sediments thicken as the basin deepens to the south into the Arkoma basin.

Deposition of Cherokee Group sediments was diverse and complicated. Sandstones in the CHB are interpreted to be fluvio-deltaic channels, reworked deltaic sands (Brenner, 1989), and valley fill successions (Walton, 1996). Coals were deposited in fluvial floodbasins, coastal plains, estuarine systems, at the end of rapid marine transgressions, and from mires that developed in Mississippian karsts (Lange, 2003).

The Cherokee group is made up of the older Krebs formation and younger Cabaniss formation that contain anywhere from 6 to 9 coals that can be seen in the subsurface and in outcrop (Woody, 1982-1985; Lange, 2003; Zeller, 1968). The Weir-Pittsuburg and Riverton coals of the Cherokee group are considered to be economically important (Newell, 2012). Coals in the Cherokee group are ~400’ to 1200’ deep and differ in maturity and lateral extent (Woody,

1982-1985). Thickness varies from 1-5 feet with vitrinite reflectance ranging from 0.5-0.7% within the Pennsylvanian group (Barker, 1992; Newell, 2012; Woody, 1982-1985).

Chapter 4 - Methods

4.1 Well Selection

Post Rock Energy Corporation provided data and access to commercial coalbed methane wells for our study. They supplied a master list of wells, a location map, and a brief summary of current water and gas production. From that list we calculated an average daily gas production and an average daily water production. We selected wells that cover a wide area spatially and had varying gas and water production characteristics (Fig. 3). My study area is located in Wilson, Neosho, Montgomery, and Labette counties (Fig. 2).

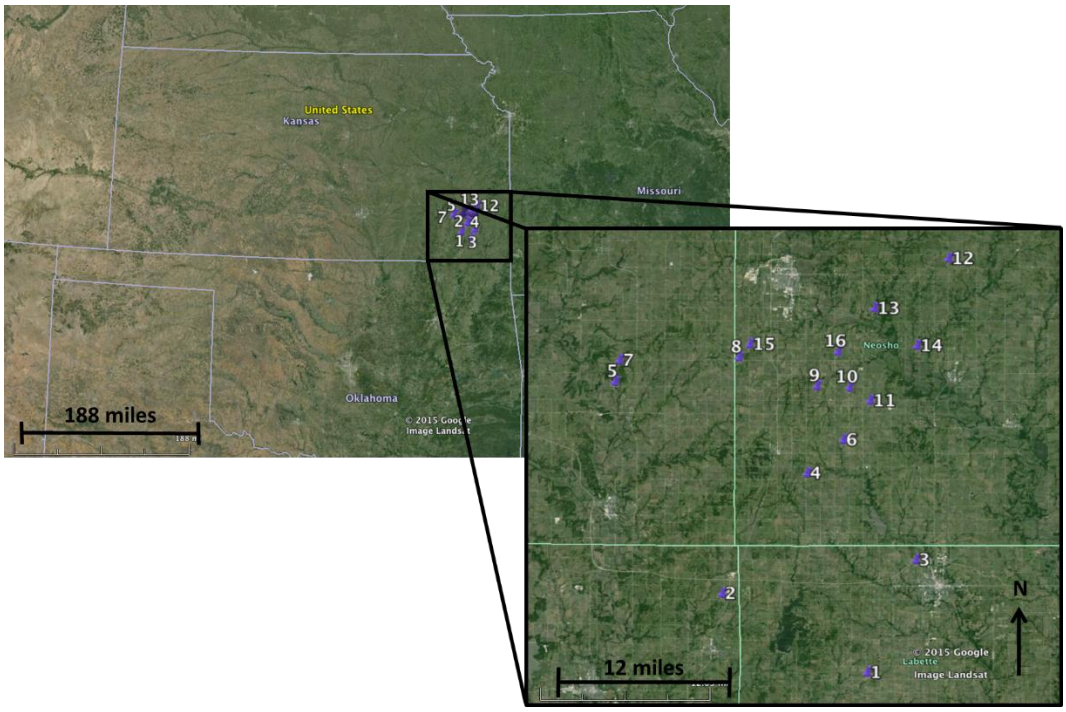

Figure 3. Well locations marked in purple with well ID's next to each marker. Satellite image taken from Google Earth.

4.2 Well Production Data

Post Rock Energy supplied detailed production data for each well that was sampled. The production data was specific to each well and not from a group of wells that fed one meter. We

summed daily production numbers for the life of the well and converted from mcf (thousand cubic feet) to mmcf (million cubic feet). Because each well produces from multiple coal zones, we were not able to constrain which coals are more prolific.

4.3 Field Methods

We collected samples during November11-13, 2013. The same data were collected at each site except for one well that was not currently producing water and one well that was producing oil with the water. Temperature, pH, and conductivity were measured in the field with an Oakton® PC300 handheld meter. Gas samples were collected in Isotubes® (Isotech Laboratories, INC.) at the well location after the produced fluid travelled through a gas separator. The gas samples were taken for compositional and isotopic analyses. Water samples were collected directly from the wellhead in sterile bottles of varying sizes for major ion chemistry and isotopic analyses. We filtered and acidified (with HCl) samples for cation analysis.

In addition to chemical analysis, we also collected water samples for culturing analysis in sterilized nitrogen-flushed serum bottles (Fig. 4). During sample collection, we attached the serum bottles directly to the well via rubber tubing and a hypodermic needle to avoid exposing the water to oxygen. Another needle was inserted into the rubber stopper of the serum bottle in order to allow disassociated gas to vent.

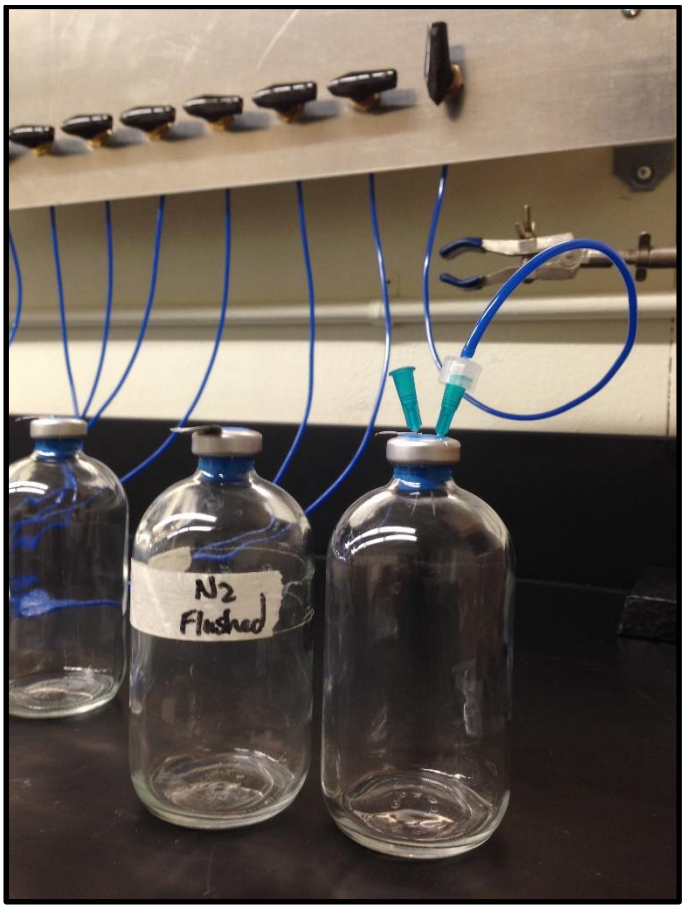

Figure 4. The serum bottle on the left has been flushed with $N_{2\,(g)}$. The serum bottle on the right is in the process of being flushed with $N_{2\,(g)}$. The needle with the blue tube attached is supplying the $N_{2\,(g)}$ and the needle without a tube attached is allowing the O_2 to vent as it is being replaced with $N_{2\,(g)}$.

4.4 Analytical Methods

We used standard methods for analysis of the major ion chemistry of our samples. We titrated samples with 0.02N H_2SO_4 to measure bicarbonate alkalinity. Major anion and cation concentrations were collected using a Dionex Corporation ICS 1100 ion chromatography (IC) system. Samples collected for ferrous iron (Fe(II)) concentrations were filtered and acidified in the field. We reduced the samples with hydroxylamine prior to analysis using the ferrozine technique (Stookey, 1970), with a Thermo Scientific Genesys 10S UV-Vis Spectrophotometer

Gas composition and isotopic samples were collected in Isotubes® and sent to Isotech Laboratories. Gas composition was measured using a gas chromatograph with accuracy of +/- 5% for C_1-C_5 and +/- 10% for C_5-C_6+. Analysis of $\delta^{13}C$ and δD of CH_4 and $\delta^{13}C$ CO_2 was done with dual inlet isotope ratio mass spectrometry (DI-IRMS). Precision of $\delta^{13}C$ is 0.1‰ and δD is 1‰. Water isotope samples were also sent to Isotech for $\delta^{18}O$ and δD of H_2O analyses using DI-IRMS. Precision for δD of H_2O is 1‰ and $\delta^{18}O$ of H_2O is 0.1‰.

In order to determine whether or not correlations are significant we used statistics. Statistical calculations were made using a Spearman's Rho calculator. For this study, P-values < 0.05 are considered statistically significant correlations.

4.5 Culturing

We tested the ability of cells to convert acetate, H_2/CO_2, and methanol into methane (Fig. 5). These three substrates represent the three major biologic pathways for methanogenesis. Each sample was also used to inoculate two control cultures: a culture that was sterilized following inoculation and a culture that was not amended with any methanogenic substrates. Each culture tube contained 10mL of formation water along with 1 mL of solution containing macronutrients (50 μM NH_4^+ and 5 μM PO_4^{3-}) and a reducing agent (100 μM Fe^{2+}). In the acetate fermentation and methyl-compound cultures, 6.3 mM acetate and 8.4 mM methanol were included as methanogenic substrates, respectively. Compositions of headspace gas in the cultures were 95% N_2 and 5% CO_2 with the exception of the H_2/CO_2 reduction cultures. In those cultures the headspace gas was composed 55% N_2, 5% CO_2, and 40% H_2.

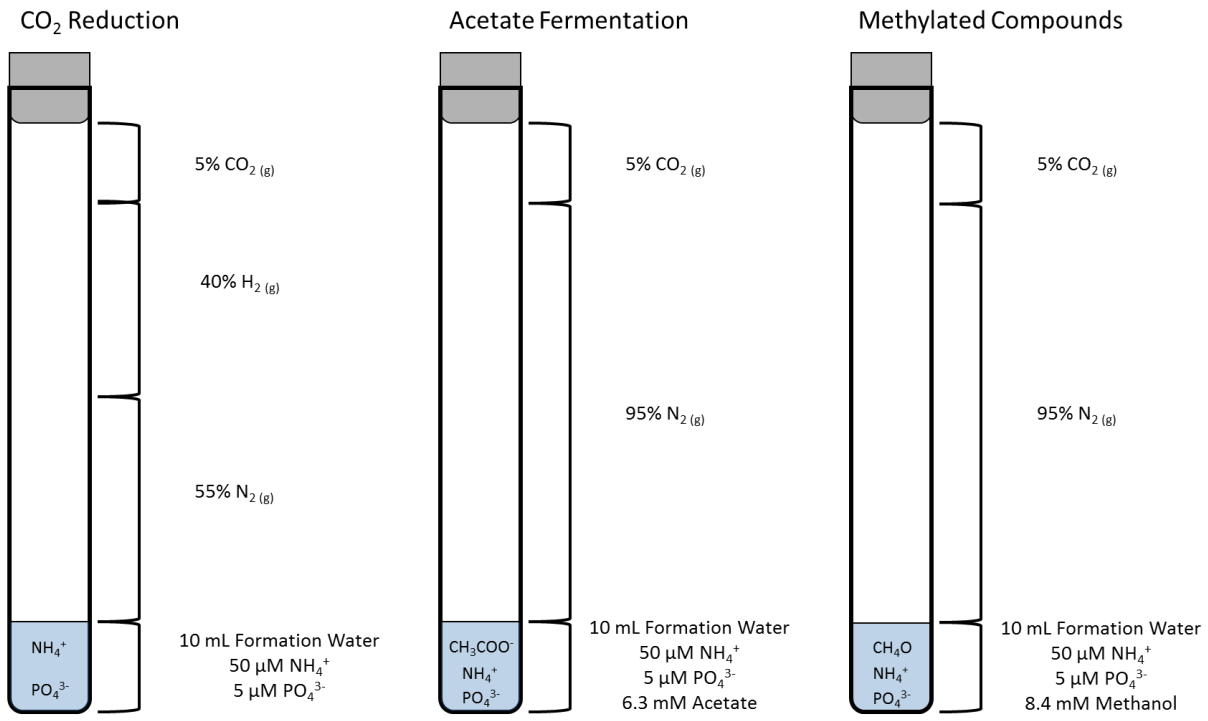

Figure 5. Diagrams of each culture scenario for the three biogenic pathways. Acetate Fermentation had added acetate to the formation water, methylated compounds had added methanol, and CO_2 reduction had added $H_{2\,(g)}$.

The concentrations of these methanogenic substrates were chosen to create an equal final abundance of CH_4 gas in the headspace (9%) if the organisms utilized all available substrate. The cultures incubated in the dark for 107 days at 21ºC. We then analyzed the methane content of the headspace of each culture using a GOW-MAC series 580 gas chromatograph.

Chapter 5 - Results

5.1 Water Chemistry

The pH, water temperature, and conductivity averaged 7.0, 19°C, and 60.9 mS/cm respectively. Alkalinity ranges from 3.33 to 8.59. Water chemistry analyzed using IC resulted in a range of concentrations (Table 2). Sampled water is Na-Cl type. The correlation between Cl^- concentration of produced water and longitude is statistically significant (P = 0.022, r = -0.059), meaning Cl^- increases westward in the basin (Fig. 6a). Since the basin dips to the west, the total depth of each well also increases to the west in a statistically significant correlation (P = 0.00005, r = -0.88). In contrast, latitude and Cl^- do not share a statistically significant correlation (P = 0.16, r = -0.38) (Fig. 6b).

Table 2. Ranges of major ion concentrations and TDS of formation water samples.

	Concentration (mg/L)			
Component	Min.	Max.	Average	Standard Deviation
HCO_3^-	203.2	518.3	300.7	91.6
Cl^-	21,300	58,540	34,267	10,493.8
Mg^{++}	346	1,912	874.5	461.2
Ca^{++}	468	2,345	1,274.4	499.6
K^+	65	184	100.5	33.3
Na^+	12,670	28,050	17,270	4,540.4
Fe^{++}	0.4	84	22.3	24.7
TDS	35,367	91,565	54,504.6	15,924.3

Water isotopes range from -35.8‰ to -50.6‰ for δD of H_2O and -5.37‰ to -7.39‰ for $\delta^{18}O$ (Appendix C). Water samples with higher $\delta^{18}O$ tend to also have higher Cl^- concentration

(P = 0.044, r = 0.525) (Fig. 7). However, they do not have a significant correlation to longitude (P = 0.15, r = -0.39). The δD H_2O does not vary significantly with Cl^- concentration (P = 0.45, r = 0.21).

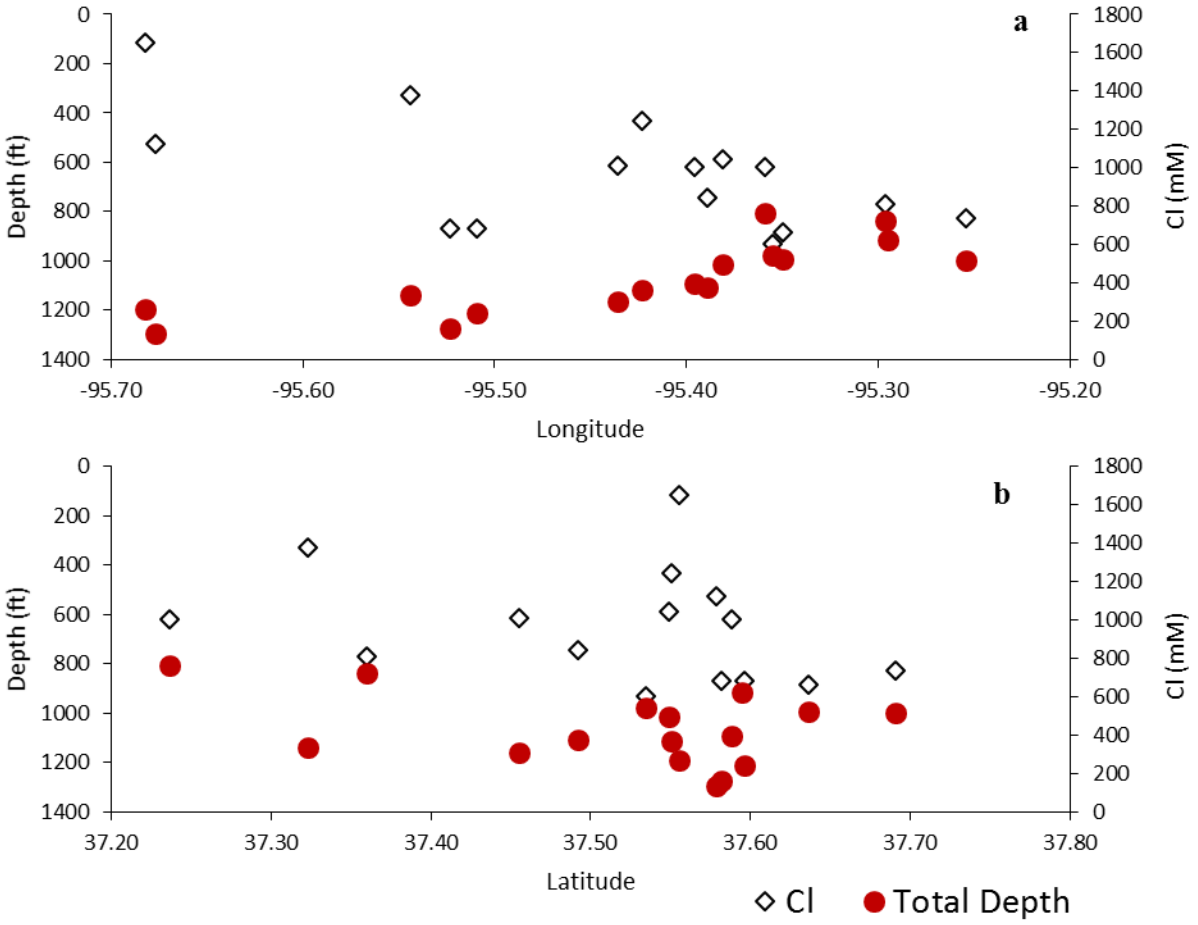

Figure 6. (a) Comparison of Cl^- content of produced water samples and total depth of sampled wells with longitude. (b) Cl^- and total depth compared to latitude.

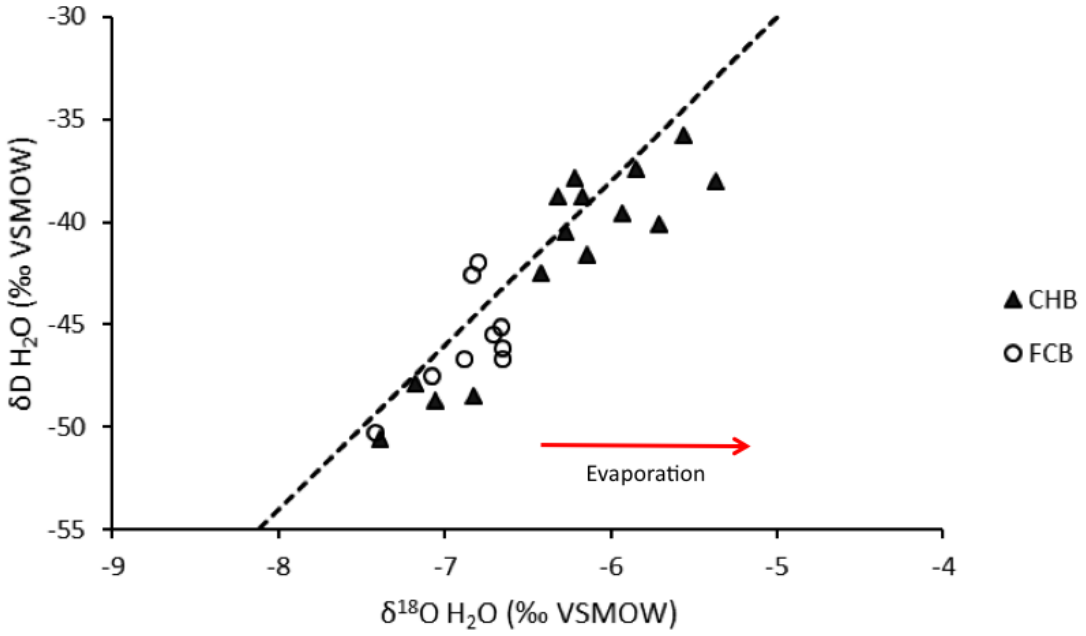

Figure 7. Comparison of $\delta^{18}O$ and δD H_2O from formation water samples. Data for the Forrest City basin (FCB) is from Cherokee group coal formation water (Mcintosh et al., 2008). Dashed line is the Global Meteoric Water Line (Craig, 1961).

5.2 Gas Isotopes & Composition

Gas samples we collected were predominantly composed of methane, consistent with dry natural gas. On average, methane, ethane, and propane abundance averaged 97.32%, 0.06%, and 0.02%, respectively. Isotopic analyses of $\delta^{13}C$ of CH_4 and CO_2 range from -56.50‰ to -69.95‰ and -0.536‰ to 9.24‰ relative to VPDB (Vienna Pee Dee Belemnite). The δD of CH_4 ranges from -217.2‰ to -228.2‰ relative to VSMOW (Vienna Standard Mean Ocean Water). The analyzed BTU ranges from 970 to 999 (Appendix B).

Comparison of gas isotopes with longitude and latitude shows two different results. There is no significant trend between $\delta^{13}C$ CH_4 with latitude (Fig. 8a). However, there is a significant correlation ($P = 0.014$) between $\delta^{13}C$ CH_4 and longitude (Fig. 8b). $\delta^{13}C$ CH_4 values increase westward in the basin.

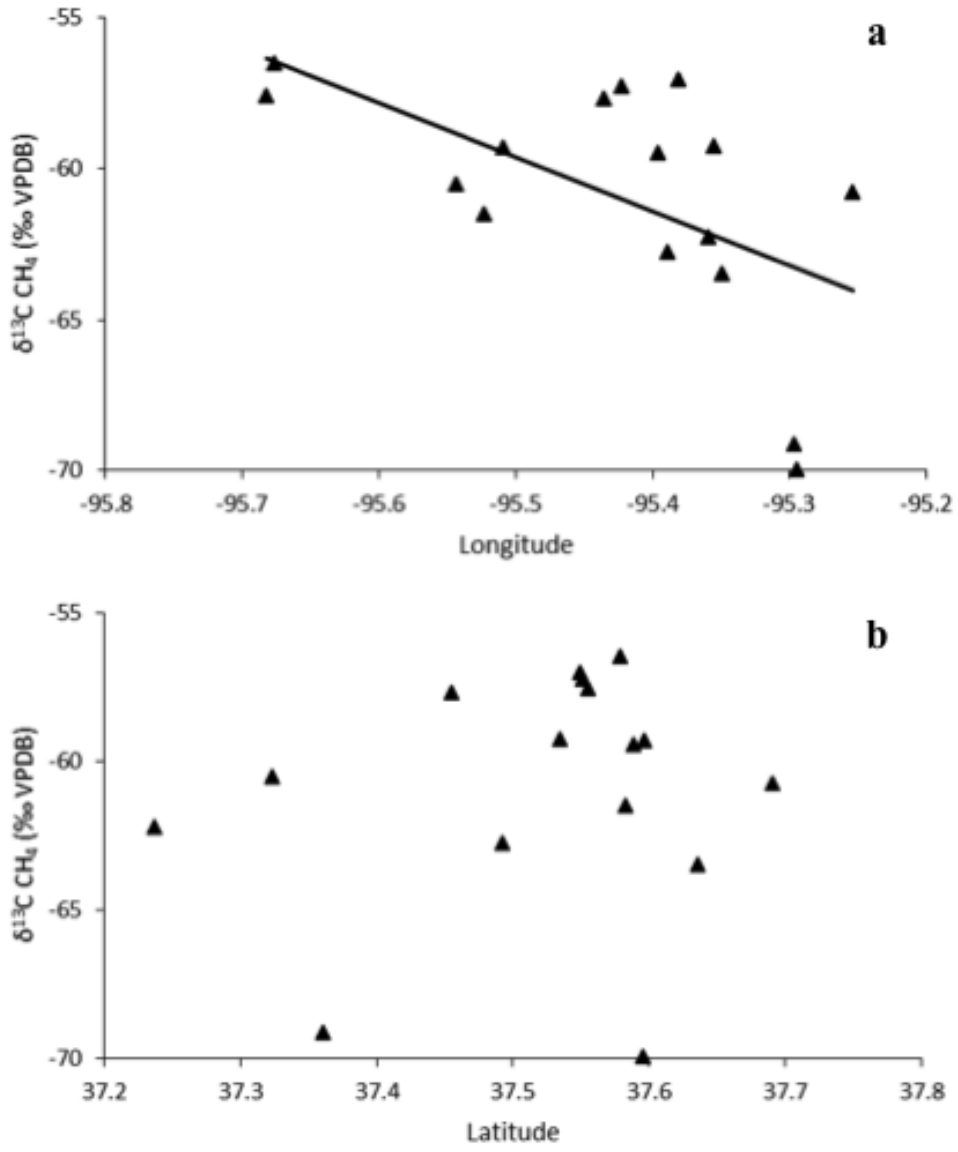

Figure 8. Comparison between (a) $\delta^{13}C$ CH_4 and longitude and (b) $\delta^{13}C$ CH_4 and latitude.

5.3 Culturing

Methane formed in live cultures inoculated with water from each well tested (Fig. 9). Conversion of hydrogen and methanol to methane was nearly uniform among the samples tested with averages 6.22% and 6.43% and standard deviations 1.15% and 0.85% respectively. By

comparison, the ability to convert acetate to methane was more variable with average 4.91% and standard deviation 3.18%. Raw data from analysis of culture headspace CH_4 is available in Appendix D.

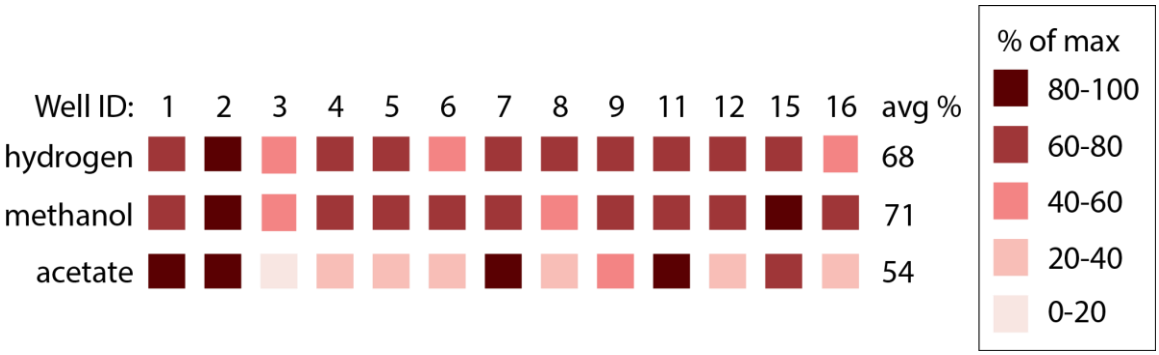

Figure 9. Heatmap depicting the abundance of methane that formed in each culture relative to the maximum amount possible. The maximum amount of CH_4 that could be produced was 9% of the headspace gas in the culture.

Chapter 6 - Discussion

6.1 Water Chemistry

Formation waters in the CHB plot similarly to the Forrest City Basin along the global meteoric water line (GMWL) (Fig. 7). Similar δD H_2O and $\delta^{18}O$ H_2O values imply that similar processes have influenced the water in each basin, consistent with the close proximity and geologic settings. For the most part, water collected from each basin tends to plot slightly to the right of the GMWL. Processes that can move water isotopic composition to the right of the GMWL include evaporation and high temperature water rock interaction. However, the extent to which either process could have influenced composition appears to be minimal considering that the data only plots slightly to the right of the GMWL.

Variation in the isotopic composition of water samples with the solute content of water suggests that variation in water isotopes may reflect mixing between dilute and saline end-members. The Cl^- concentration and $\delta^{18}O$ of our samples share a significant positive correlation ($P = 0.044$, $r = 0.525$) (Fig. 10). This trend is consistent with dilution of an isotopically heavy saline brine with water that is isotopically lighter and lower in solute content. Similar relationships have been observed in the Illinois Basin where meteoric re-charge reaches the New Albany shale and Pennsylvanian coals to mix with basin brines (Schlegel et al., 2011). In contrast, Cl^- negatively correlated with the $\delta^{18}O$ in samples collected by McIntosh et al. (2008) in the FCB. McIntosh et al. suggested that the trend in their samples might reflect climatic shifts and variable residence times. Salinity in our samples have levels lower than those observed in other biogenic gas reservoirs (Waldron et al., 2007)

In addition to the trend between water isotopes and salinity, the trend between Cl^- content and total well depth is consistent with results observed in the Illinois and Michigan basin

(Martini, 1998; McIntosh et al., 2002). This relationship may reflect a decrease with depth in the proportion of freshwater recharge that has mixed with basin brine and/or dissolution of evaporite minerals at depth within the basin. Cl^-/Br^- ratios of our samples are relatively low, however, suggesting that interaction with evaporate deposits is limited (Appendix C). Hence, an increasing component of brine with depth is a more likely explanation.

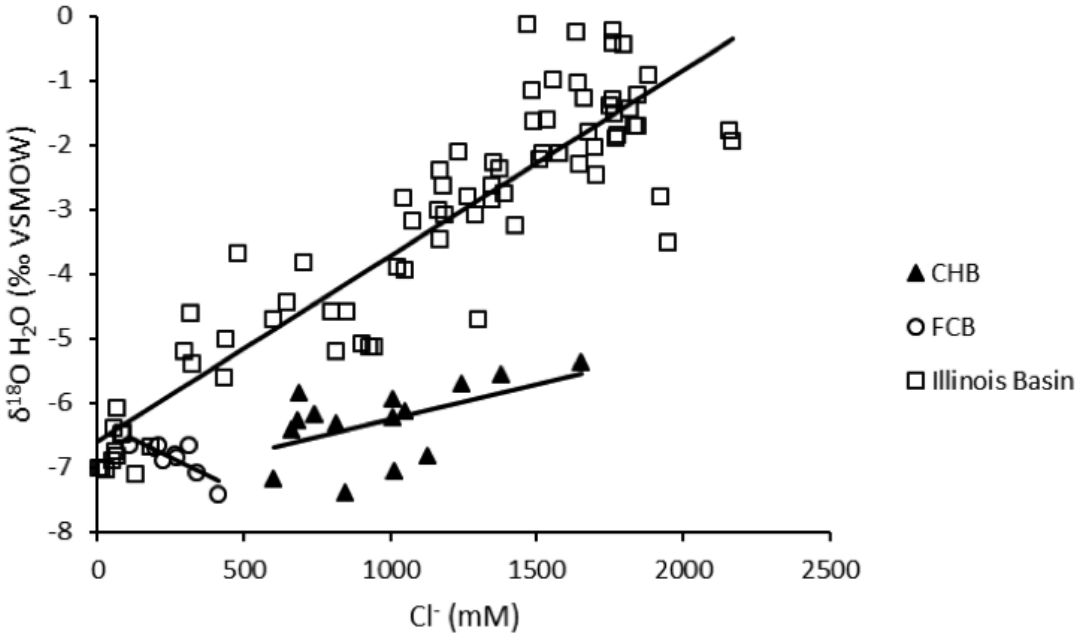

Figure 10. Chloride concentrations plotted against δO^{18} for the CHB (this study), the FCB (McIntosh et al., 2008), New Albany shale and Pennsylvanian coals from the Illinois basin (Schlegel et al., 2011). Black lines through each dataset are lines of best fit.

Stable carbon isotopes of HCO_3^- (DIC) compared to formation water alkalinity indicates whether or not microbial methanogenesis is altering the values of $\delta^{13}C$ DIC in the water. Methanogens will selectively use isotopically lighter portions of the formation water, which leaves behind water that is enriched in heavier isotopes. Therefore, a comparison of $\delta^{13}C$ DIC and alkalinity can show whether microbial methanogenesis has taken place or not (Fig. 11). The

FCB has a stronger correlation of increasing alkalinity with increased $\delta^{13}C$ DIC than the CHB. Data from the CHB more closely resembles that of the Antrim and New Albany shales of the Michigan and Illinois basins, respectively (Mcintosh et al., 2002; Martini et al., 1998). The Antrim and New Albany shales retain low alkalinities (< 10 meq/L) until $\delta^{13}C$ DIC is > 20‰, which is similar to the CHB. The $\delta^{13}C$ DIC in the CHB gets heavier, which is consistent with H_2/CO_2 reduction, but not at the same level of alkalinity production as other basins. The important point of this comparison is that the large $\delta^{13}C$ DIC in our samples is consistent with microbial methanogenesis. This is not an unreasonable assumption when considering salinity in our samples have levels lower than those observed in other biogenic gas reservoirs, like in Waldron et al., 2007. Indicating that formation water salinity is within the limits for microbial methanogenesis.

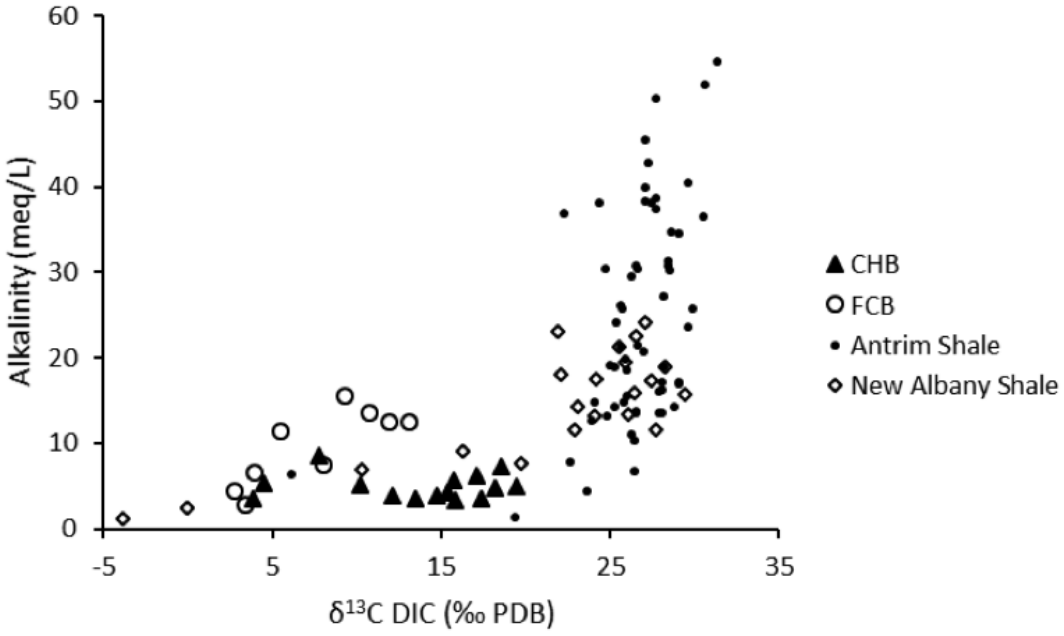

Figure 11. Values for the $\delta^{13}C$ DIC and alkalinity of waters from the FCB (McIntosh et al., 2008), Antrim Shale Michigan Basin (Martini, 1998), New Albany Shale Illinois Basin (McIntosh et al., 2002), and CHB (this study). Each basin is interpreted to be a biogenic reservoir.

6.2 Pathway of Methanogenesis

Gas chemistry and isotopic composition can be used to evaluate how natural gas formed. We used a Bernard plot (Bernard, 1978), a traditional approach that compares gas dryness index [$C_1/(C_2+C_3)$] to $\delta^{13}C$ CH_4, to determine whether the produced gas was biogenic or thermogenic in origin (Fig. 12). Microbial gas tends to be dry, even though there are microorganisms that can make longer chain hydrocarbons, because microbes that make methane are more abundant in methanogenic communities (Head, 2014). On the other hand, thermocatalytic reactions more readily make longer chain hydrocarbons (i.e. wet gas). The composition of gas samples is consistent with gas that is produced biologically with a small contribution of thermogenic gas mixed into the biogenic gas.

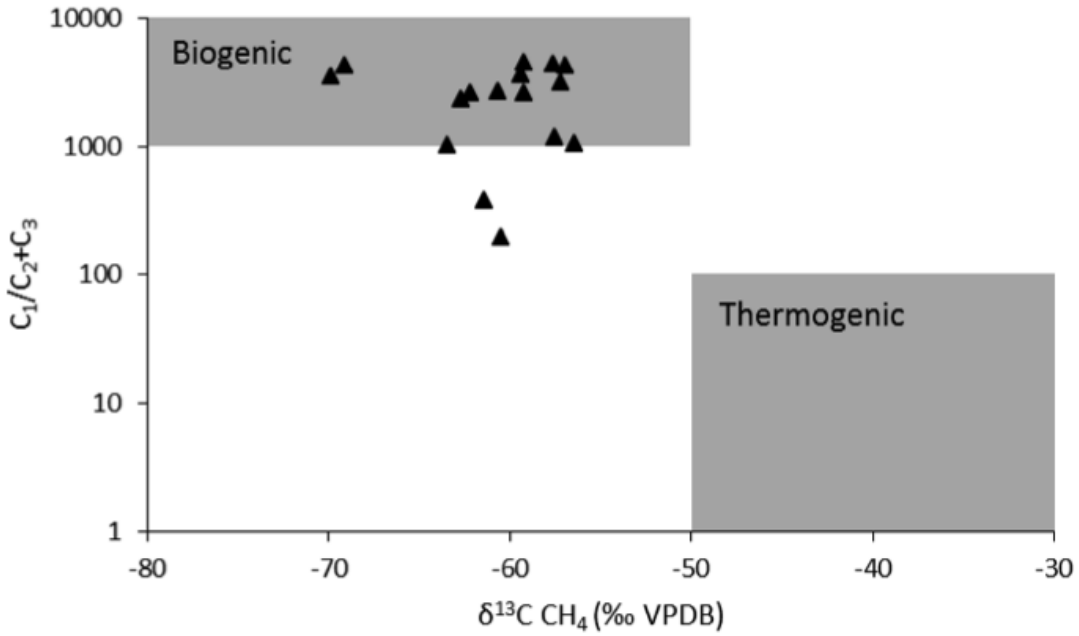

Figure 12. Bernard plot used to determine gas origin in the CHB by comparing gas dryness index and $\delta^{13}C$ of CH_4.

A further evaluation of how microbes formed gas in our samples was done using a Whiticar plot, which compares the $\delta^{13}C$ and δD of CH_4 (Fig. 13) (Whiticar et al., 1986). Values

from the CHB plot in the H_2/CO_2 reduction zone with a small contribution of thermogenic gas, which is consistent with the Bernard plot.

Previous work had used these traditional plots to evaluate gas origin in CHB coalbeds (Newell and Carr, 2009). Newell and Carr interpreted that some of the gas is thermogenic and assumed that it likely migrated from the Arkoma basin, directly to the south (Newell, 2012). Considering the thermal maturity and presence of black shales in the basin, the small contribution of thermogenic gas could also have originated within the basin.

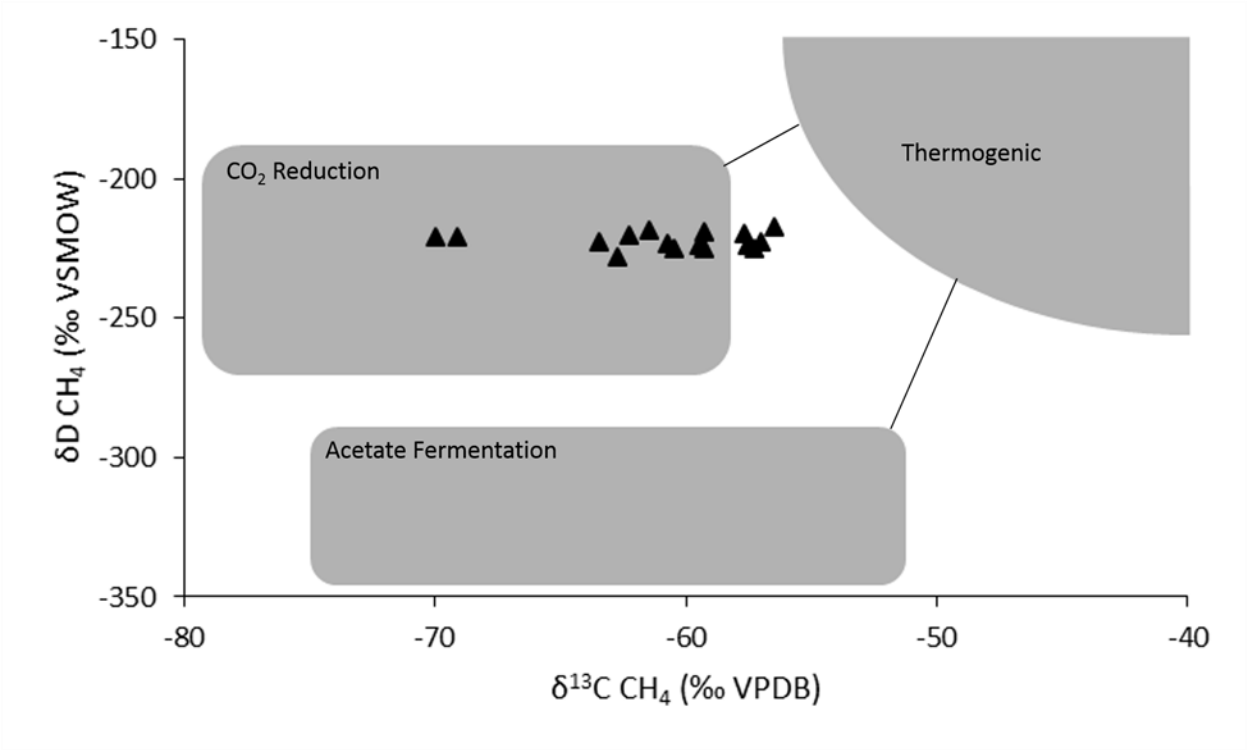

Figure 13. Comparison of $\delta^{13}C$ and δD CH_4 to determine specific methanogenic pathway. Gas isotopes can differentiate H_2/CO_2 from acetate/methyl, but it cannot distinguish acetate fermentation from methylotrophic methanogenesis.

Two additional isotopic tracers, which are thought to be more widely applicable, were used to evaluate the origin of the gas (Golding, 2013). The first was to compare the $\delta^{13}C$ CH_4 to that of $\delta^{13}C$ CO_2 in the same sample (Fig. 14). This plot was done with calculated fractionation

factor ($\alpha_c = (\delta^{13}C\ CO_2 + 1000)/(\delta^{13}C\ CH_4 + 1000)$) lines to separate zones for H_2/CO_2 reduction and acetate fermentation (Whiticar et al., 1986). The CHB data plots within the range for H_2/CO_2 reduction, $\alpha_c > 1.06$ (Golding, 2013). A line of best fit drawn for the data shows that as $\delta^{13}C\ CH_4$ gets heavier it approaches the $\alpha_c = 1.06$ line. This means that it is approaching the zone representative of acetate fermentation. While the primary pathway of methanogenesis is H_2/CO_2 reduction, there seems to be some potential contribution of acetate fermentation in the CHB.

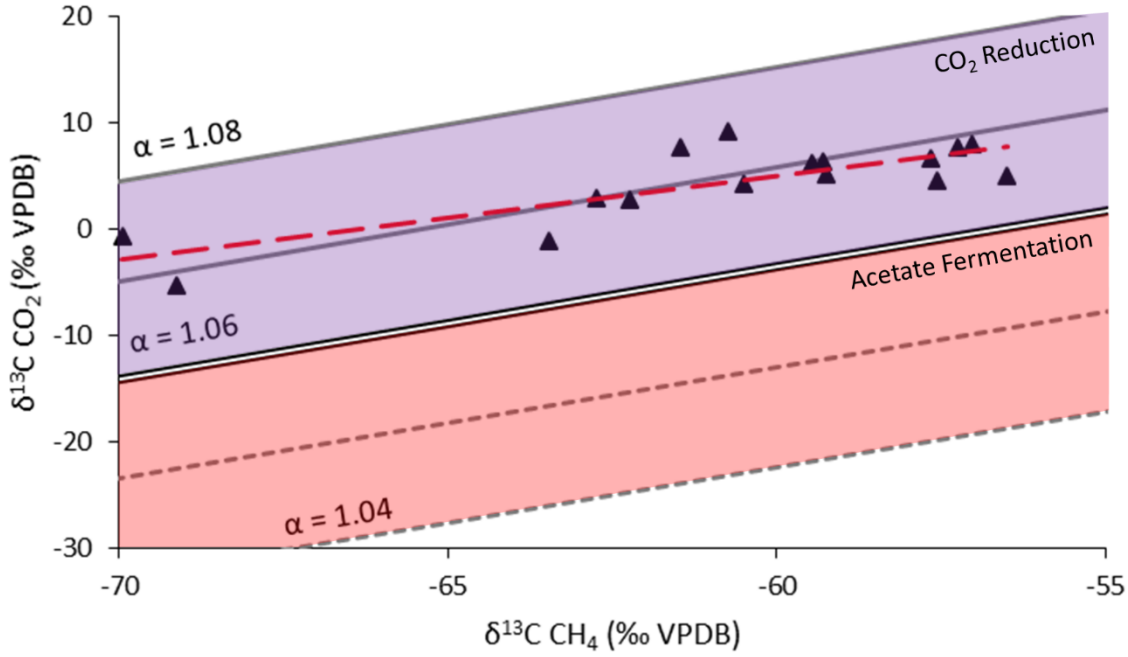

Figure 14. This comparison between $\delta^{13}C\ CH_4$ and $\delta^{13}C\ CO_2$ for the CHB was plotted with α_c lines to determine the methanogenic pathway. Red dashed line is the best fit line for CHB samples. Values in purple region are indicative of CO_2 reduction and values in red region are indicative of acetate fermentation.

The second tracer for methane origin is the comparison of the δD of co-produced water with the δD of CH_4. Whiticar (1999) defined a line for H_2/CO_2 reduction:

$$\delta D_{CH4} = \delta D_{H2O} - 160‰$$

The equation for H_2/CO_2 reduction assumes that 100% of H^+ ions required for CH_4 formation are sourced from the water where the microbes live. Multiple environments have shown to generate methane roughly 160-180‰ less than the hydrogen isotopes of formation water (Whiticar, 1999). A line for acetoclastic or methylotrophic methanogenesis (acetate/methyl) is defined by the equation:

$$\delta D_{CH4} = 0.25*\delta D_{H2O} - 300‰$$

It is difficult to determine the difference between acetoclastic or methylotrophic methanogenesis due to the variability of hydrogen isotopes in acetate and methylated compounds. Known δD values for CH_4 formed from acetate or methyl groups are 300‰-377‰ less than δD of formation water (Whiticar, 1999). Acetate/methyl are grouped together when using isotopic tracers, because of the δD_{CH4} variability. Sampled wells plot near the H_2/CO_2 reduction line at lighter δD H_2O, but move away from the line at heavier δD H_2O (Fig. 15).

A calculation of potential contribution was done to help determine what percentage of produced methane was from the different pathways. Assuming that the -300‰ line is 100% acetate/methyl methanogenesis and the -160‰ line is 100% H_2/CO_2 reduction, a potential percent contribution was determined. The distance between line A and B in δD CH_4 at each samples δD H_2O value was calculated and then the position of each sample along the line was used to determine the potential influence of the different pathways. Acetate/methyl contribution on average is 18.75% and the contribution of H_2/CO_2 reduction is 81.25%. Samples with lighter δD H_2O values have a larger potential contribution of acetate/methyl formation. Both isotopic tracers have shown that the primary methanogenic pathway is H_2/CO_2 reduction with some contribution of acetate/methyl methanogenesis.

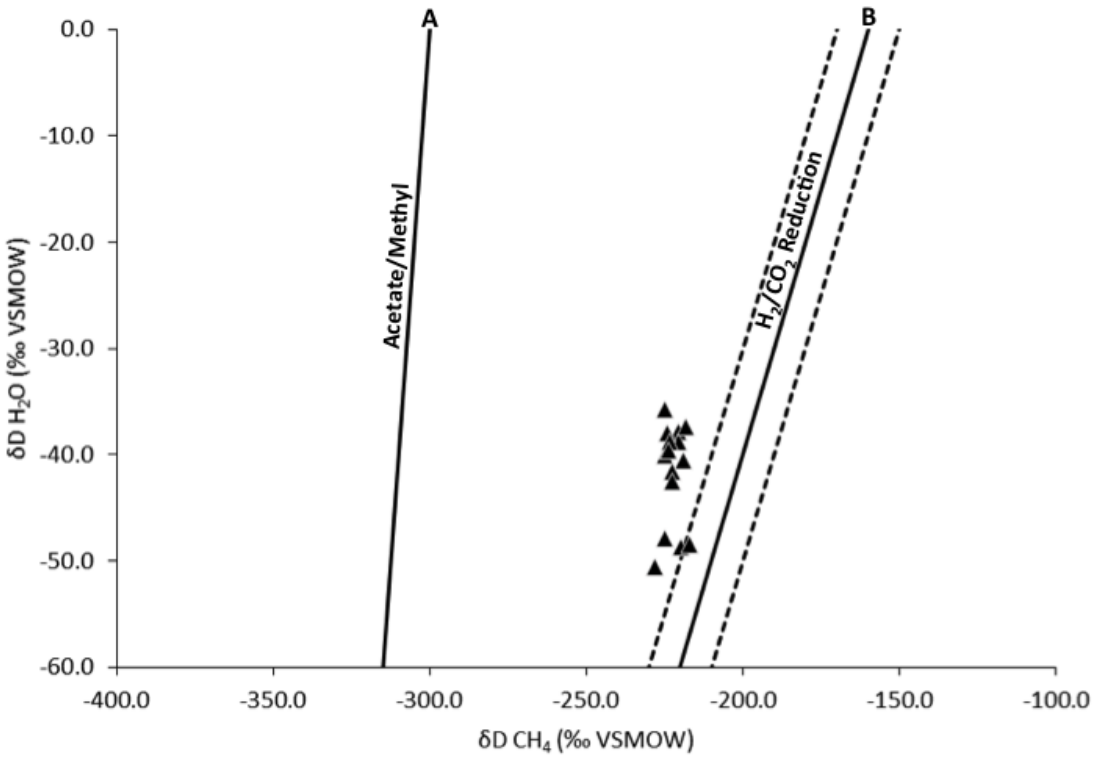

Figure 15. Comparison of δD CH_4 and H_2O with predetermined lines of methanogenic pathways from Whiticar (1999). Line (A) is representative of CO_2 reduction with dashed lines indicating 160‰ +/- 10‰ and line (B) is representative of acetate/methyl methanogenesis.

The separation of data points from the -160‰ line (Fig. 15) could be interpreted in two ways. The δD of CH_4 does not vary with the δD H_2O. Or, as the δD of H_2O values increase, the data trend begins to shift towards the acetate/methyl line and could be indicative of added acetate/methyl contribution to methanogenesis. The increase in δD H_2O values alone does not explain the shift away from the H_2/CO_2 reduction line. A study by Waldron et al. (2007) showed that formation water salinity was a driving factor for microbial community composition in the Antrim Shale of the Michigan Basin. It also showed that some hydrogenotrophic communities adapted to salinities above the previously determined upper limit (Waldron et al., 2007). In the CHB the δD H_2O values increase with salinity. This relationship between salinity and

community composition could explain why the CHB shifts towards the acetate/methyl line at heavier δD H_2O.

6.3 Formation water geochemistry and methanogenesis

We calculated isotope separation of the carbon isotopes ($\Delta^{13}C_{CO2\text{-}CH4} = \delta^{13}CO_2 - \delta^{13}CH_4$) and hydrogen isotopes ($\Delta D_{CH4\text{-}H2O} = \delta D\ CH_4 - \delta D\ H_2O$) to evaluate how methanogenic pathways relate to geochemistry. The $\Delta^{13}C$ values range from 61.52‰ to 69.99‰ and the ΔD values range from -168‰ to -189.1‰. Golding (2013) defined ranges of isotope separation for the H_2/CO_2 reduction pathway and the acetate/methyl pathways. The range for the acetate/methyl pathway using ΔD had to be calculated using the equation $\delta D_{CH4} = 0.25*\delta D_{H2O}$ - 300‰. Using two variations of the equation subtracting 300‰ and 325‰, with multiple δD_{H2O} values across the sample range, we calculated pseudo δD_{CH4} values that correlate to acetate/methyl methanogenesis. We determined a range of isotope fractionation factors for acetate/methyl methanogenesis by averaging the calculated ΔD values.

We plotted the $\Delta^{13}C$ and ΔD values against Cl^- to evaluate whether our data are consistent with salinity as a control on methanogenic pathway (Fig. 16 & 17). The $\Delta^{13}C$ values show that H_2/CO_2 reduction is predominate throughout the basin (Fig. 16). Values are located at the lower boundary in the range for H_2/CO_2 reduction and decrease with increasing Cl^- concentrations indicating that there could be some acetate/methyl contribution. The ΔD values plot isotopically lighter than the H_2/CO_2 reduction boundaries and decrease with increasing Cl^- concentration (Fig. 17). The CHB seems to demonstrate that a community of acetoclastic methanogens could be increasing at salinities above the known upper limit of ~1,000 mM Cl^-.

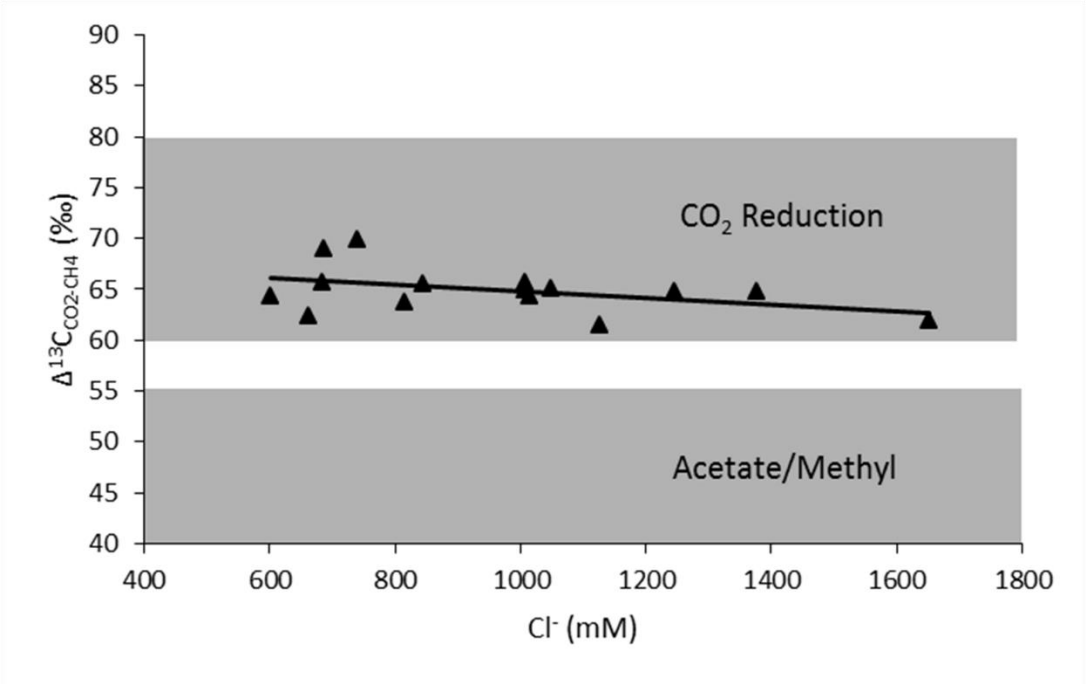

Figure 16. Carbon isotope fractionation plotted against CHB Cl- concentration. Grey shaded areas are representative of fractionation ranges that correlate to CO_2 reduction and Acetate/methyl methanogenesis.

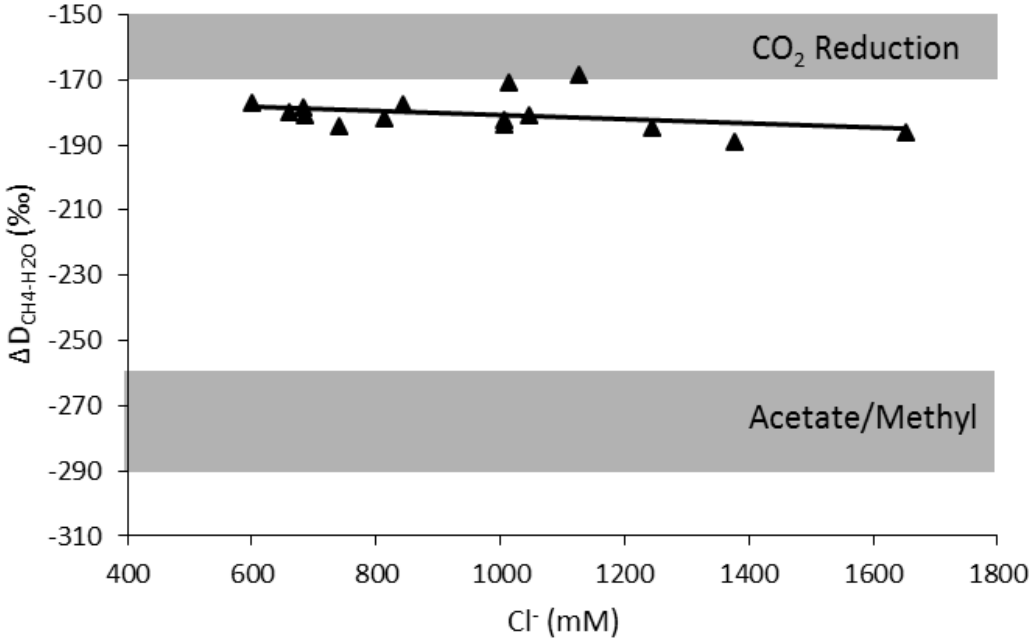

Figure 17. Hydrogen isotope fractionation plotted against CHB Cl^- concentration. Grey shaded areas are representative of fractionation ranges that correlate to CO_2 reduction and Acetate/methyl methanogenesis.

These results are somewhat unexpected. Traditionally, acetate fermentation coincides with freshwater environments and H_2/CO_2 reduction is more common in saline environments. However, in our samples we see an increase in the amount of acetate or methyl contribution with salinity. We know our samples are within salinity limits (~2,000 mM) (Whiticar et al., 1986) for methanogenic bacteria to live so it is not unreasonable to assume that acetoclastic (or methylotrophic) methanogens could be contributing to methanogenesis at higher salinity environments. Therefore, the shift in δD CH_4 towards the acetate/methyl line is likely due to a change in microbial communities with increasing Cl^- concentrations rather than the changes in the isotopic composition of water itself.

The fractionation factor for carbon isotopes (α_c) was compared to longitude to understand spatial correlations to gas isotopes. Sampled gas α_c decreases westward in the basin (Fig. 18). While the correlation is not statistically significant ($p = 0.187$), the fractionation factor does seem to decrease towards the acetate/methyl pathway westward in the basin. This is the same trend we see with $\Delta^{13}C$ and chloride concentrations, further supporting the interpretation that microbial communities are shifting towards acetate/methyl with depth, increased Cl^-, and location in the basin.

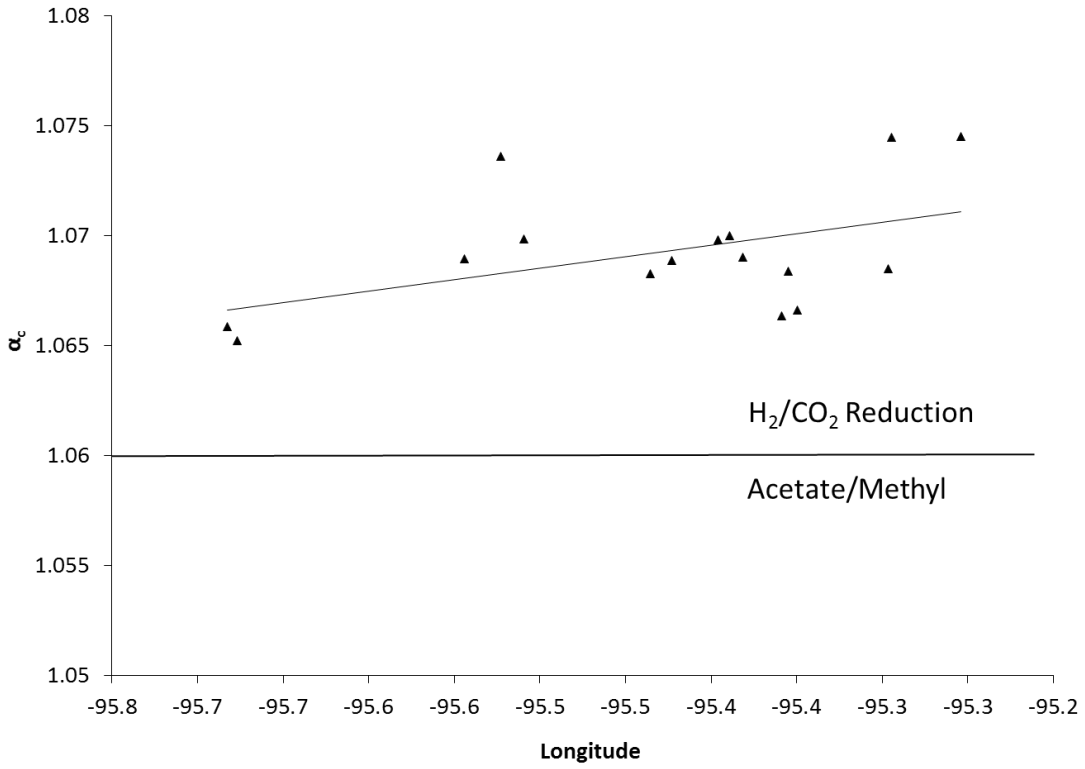

Figure 18. Fractionation factor of carbon isotopes compared to longitude. The line at α_c = 1.06 indicates the divider between H2/CO2 reduction and acetate/methyl.

6.4 Analysis of Production

In order to determine geological controls on production, we compared cumulative production to the total number of feet of coal that were perforated in each well (Fig. 19). This was done to determine if gas production in the CHB is dependent upon coal thickness or not. While there is no statistical correlation between the data, the gas production does seem to decrease with increasing amount of open perforations. This could be due to the presence or lack of prolific coals, the age differences between different wells, or each wells stage in the de-watering process. This negative correlation is evidence that increased thickness of coal perforated in each well does not increase production.

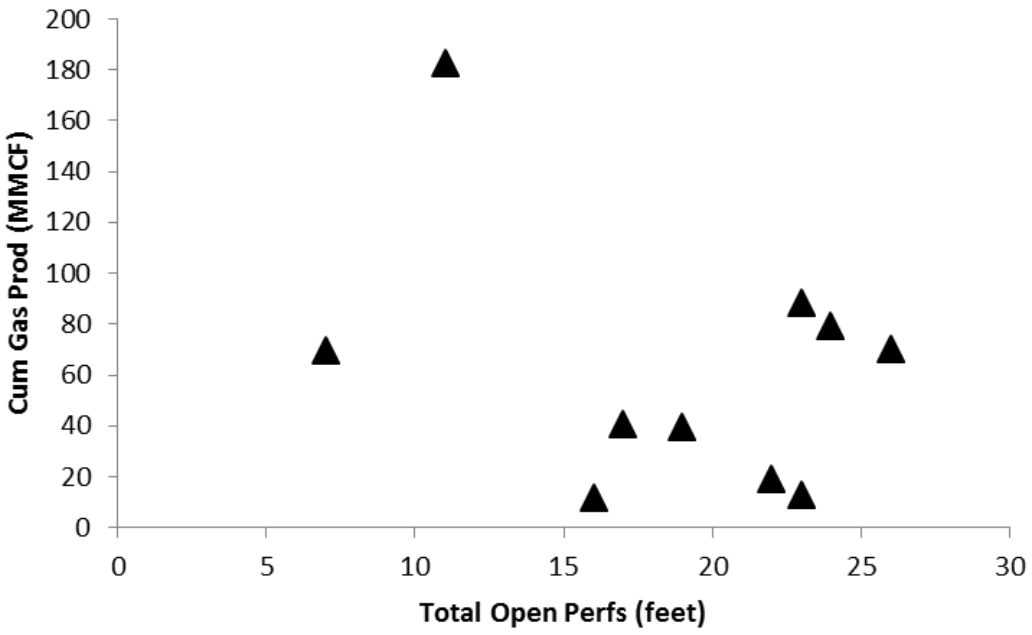

Figure 19. Total open perforations (perfs) compared to cumulative gas production in million cubic feet.

Sodium and chloride are the major contributors to TDS in the CHB and are potentially the controlling factors for microbial communities. Because Cl^- is an important chemical constituent, it was compared to cumulative gas production to determine if there is any geochemical control on production (Fig. 20). As Cl^- concentration increases, cumulative production decreases. This correlation matches the shift from H_2/CO_2 reduction to acetate/methyl contribution. Potentially, the decreased contribution from H_2/CO_2 reduction also decreases the cumulative production of the well. While this correlation is not very strong, it does seem to exist in the field.

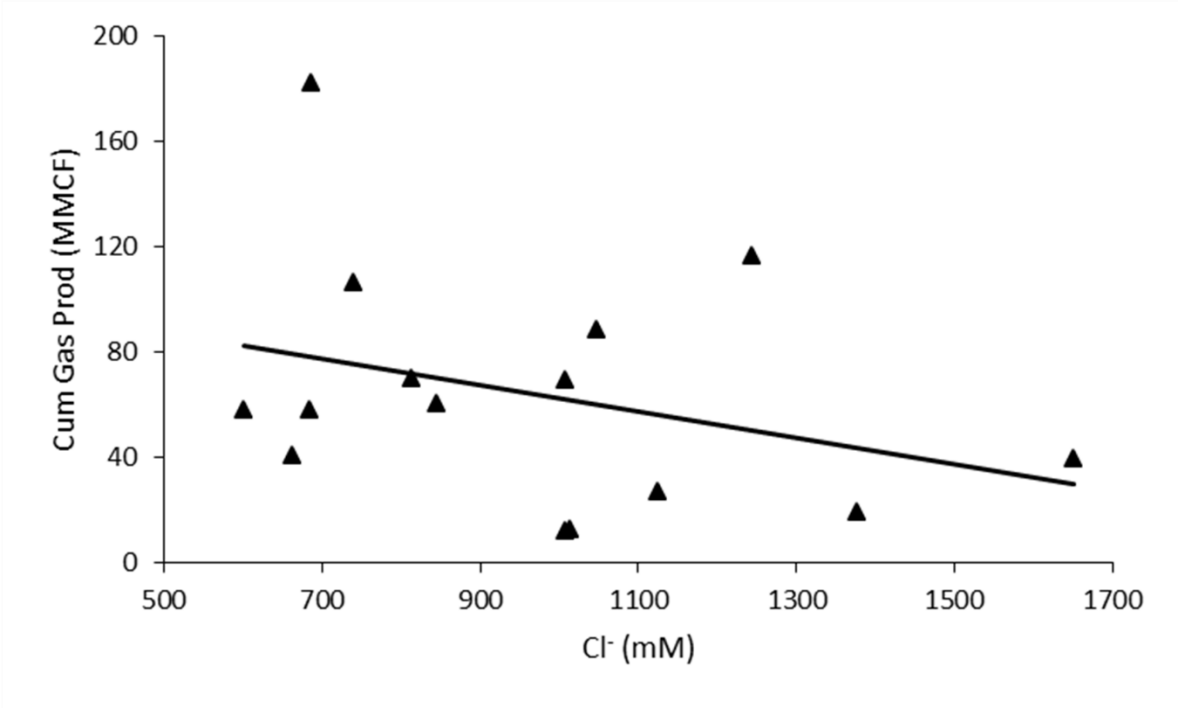

Figure 20. Comparison of Cl^- to cumulative gas production for the CHB. The solid black line is the line of best fit for the samples.

We compared Fe^{2+} to average gas production from two weeks prior to sampling (Fig. 21) in order to determine the redox state of the produced water and how it correlates to gas production. There is a statistically significant (P = 0.011) correlation between Fe^{2+} concentration and gas production. In samples with high gas production, there is an increased amount of ferrous iron when compared to samples with lower gas production. The variation in Fe^{2+} concentrations of sampled water could indicate that the water is in a reducing environment. Because larger concentrations of Fe^{2+} correlate to higher gas production, reduction of Fe^{3+} could be important for increased production of gas. The varying quantities of Fe^{2+} could also be indicative of different sources of water. However, different sources of water are unlikely considering the previous correlations found between water chemistry and isotopes in this study.

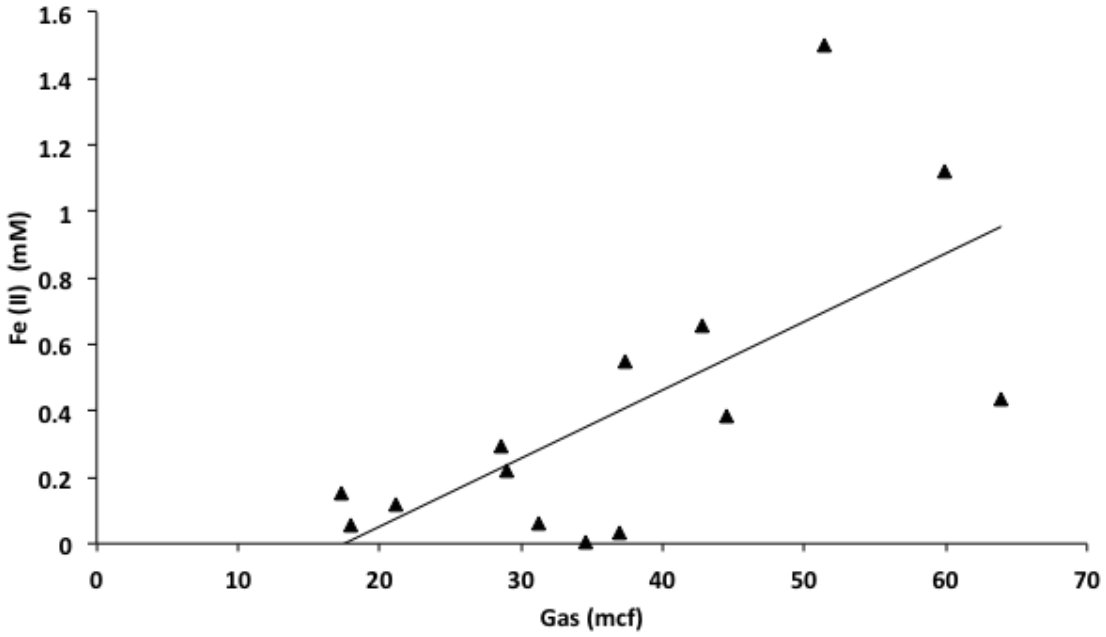

Figure 21. Comparison of average gas production from the two weeks prior to sampling and ferrous iron concentration (Fe^{2+}). Production increases with increasing iron concentration.

More detailed comparisons between production and formation water geochemistry could not be made because of the number of uncontrollable variables in production information; each well produces from multiple or different coal seams, are different ages, and in different stages of de-watering. Because of these reasons, it is difficult to determine specific correlations between geochemistry and production in the CHB.

Chapter 7 - Conclusions

This study aimed to test the research hypotheses that (1) a portion of the gas in Cherokee Basin coalbeds was produced biologically and (2) formation water geochemistry influences gas production. These hypotheses were tested with a field study and lab experiments that utilized formation water, gas samples, and all available production data. The conclusions we reached are as follows:

1. Consistent with the relative low thermal maturity of Cherokee Basin coalbeds, natural gas in the field area is primarily biogenic in origin. Isotopic results indicate that microorganisms formed the gas primarily through CO_2 reduction.
2. A small component of gas formed via acetoclastic or methylotrophic methanogenesis. The proportion of gas formed by these alternative pathways appears to increase with the solute content of the water.
3. Culturing results demonstrate that living cells present in the basin are able to make methane.
4. Production does not clearly relate to total coal thickness per well or produced water geochemistry for the most part. Additional research is needed to explore whether those variables may influence production rates.

References

Barker, C.E., Goldstein, R.H., Hatch, J.R., Walton, A.W., Wojcik, K.M., 1992. Burial history and thermal maturation of Pennsylvanian rocks, Cherokee basin, southeastern Kansas: *Oklahoma Geological Survey Circular,* Vol. 93, pp. 299-310.

Bernard, B.B., Brooks, J.M., Slackett, W.M., 1978. Light hydrocarbons in recent Texas continental shelf and slope sediments: *J. Geophys. Res.,* Vol. 83, pp. 4053-4061.

Brenner, R.L., 1989. Stratigraphy, petrology, and paleogeography of the upper portion of the Cherokee Group (Middle Pennsylvanian), eastern Kansas and northeastern Oklahoma: *Kansas Geological Survey Geology Series* 3, 69 p.

Craig, Harmon, 1961. Isotopic variations in meteoric waters: *Science*, Vol. 133, No. 3465, pp. 1702-1703.

Dow, W.G., O'Connor, D.I., 1982. Kerogen maturity and type by reflected light microscopy applied to petroleum exploration: *The Society of Economic Paleontologists and Mineralogists (SEPM) How to Assess Maturation and Paleotempuratures* SC7, pp. 133-157.

Golding, S.D., Boreham, C.J., Esterle, J.S., 2013. Stable isotope geochemistry of coal bed and shale gas and related production waters: A review: *International Journal of Coal Geology,* Vol. 120, pp. 24-40.

Head, I.M., Gray, N.D., Larter, S.R., 2014. Life in the slow lane; biogeochemistry of biodegraded petroleum containing reservoirs and implications for energy recovery and carbon management: *Frontiers in Microbiology,* Vol. 5, Article 566. 23p.

Lange, J.P., 2003. Stratigraphy, depositional environments and coalbed methane resources of Cherokee Group coals (Middle Pennsylvanian) – southeastern Kansas: *Kansas Geological Survey Open-File Report* 82, 158p.

Ley, H.A., 1935. Natural gas in eastern Kansas: *AAPG Special Volumes* 7, pp. 483-509.

Martini, A.M., Walter, L.M., Budai, J.M., Ku, T.C.W., Kaiser, C.J., Schoell, M.,1998. Genetic and temporal relations between formation waters and biogenic methane: Upper Devonian Antrim Shale, Michigan basin, USA: *Geochimica et Cosmochimica Acta,* Vol. 62, No. 10, pp. 1699-1720.

McIntosh, J.C., Walter, L.M., Martini, A.M., 2002. Pleistocene recharge to midcontinent basins: Effects on salinity structure and microbial gas generation: *Geochimica et Cosmochimica Acta*, Vol. 66, No. 10, pp. 1681-1700.

McIntosh, J., Martini, A., Petsch, S., Huang, R., Nusslein, K., 2008. Biogeochemistry of the Forest City basin coalbed methane play: *International Journal of Coal Geology,* Vol. 76, No. 1-2, pp. 111-118.

Merriam, D.F., 1963. The geologic history of Kansas. *Kansas Geological Survey Bulletin* 162.

Newell, D.K., Carr, T.R., (2009), in Carr, T., D'Angostino, T., Ambrose W., Pashin, J., and Rasen, N.C. (eds), "Coal-Bed Natural Gas Production and Gas Content of Pennsylvanian Coal Units in Eastern Kansas" Proceedings of the 29th Annual Gulf Coast Section, SEPM, Bob F. Perkins Research Conference, Houston, Tx, *Unconventional Energy Resources; Making the Unconventional Conventional*, p. 353-383.

Newell, D.K., 2010. Fall may be imminent for Kansas Cherokee basin coalbed gas output: *Oil & Gas Journal*, pp. 33-40.

Newell, D.K., 2012. Personal Communication: Personal unpublished writings and ideas were transferred and conveyed through e-mail.

Schlegel, M.E., McIntosh, J.C., Bates, B.L., Kirk, M.F., Martini, A.M., 2011. Comparison of fluid geochemistry and microbiology of multiple organic-rich reservoirs in the Illinois basin, USA: evidence for controls on methanogenesis and microbial transport: *Geochimica et Cosmochimica Acta* 75, pp. 1903-1919.

Sutherland, P.K., 1988. Late Mississippian and Pennsylvanian depositional history in the Arkoma basin area, Oklahoma and Arkansas: *Geological Society of America Bulletin*, Vol. 100, pp. 1787-1802.

Stookey, L.L., 1970. Ferrozine – a new spectrophotometric reagent for iron: *Anal. Chem.* 42, pp. 779-781.

"U.S. Energy Information Administration - EIA - Independent Statistics and Analysis." U.S. Crude Oil, Natural Gas, and Natural Gas Liquids Proved Reserves. Dec. 2014.

Waldron, P.J., Petsch, S.T., Martini, A.M., Nüsslein, K., 2007. Salinity constraints on subsurface archaeal diversity and methanogenesis in sedimentary rock rich in organic matter: *Applied and Environmental Microbiology*, Vol. 73, No. 13, pp. 4171-4179.

Walton, A.W., 1996. Sequences in the Cherokee Group (Desmoinesian, Middle Pennsylvanian) of southeastern Kansas: *Transactions of the 1995 AAPG Mid-Continent Section Meeting*.

Whiticar, M.J., Faber, E., Schoell, M., 1986. Biogenic methane formation in marine and freshwater environments-CO_2 reduction vs. acetate fermentation isotope evidence: *Geochemica et Cosmochimica Acta* 50, pp. 693-709.

Whiticar, M.J., 1999. Carbon and hydrogen isotope systematics of bacterial formation and oxidation of methane: *Chemical Geology*, Vol. 161, No. 1-3, pp. 291-314.

Woody, M.D., 1982-1985. Sedimentology, diagenesis, and petrophysics of selected Cherokee Group (Desmoinesian) sandstones in southeastern Kansas: *OCGS – The Shale Shaker Digest XI* 33-35, pp. 244-273.

Zeller, D. E., Jewett, J.M., Bayne, C.K., Goebel, E.D., O'Connor, H.G., Swineford, A., 1968. The stratigraphic succession in Kansas: *Kansas Geological Survey Bulletin* 189.

Appendix A - Basic well information

Sample #	Sample Name	API #	Spud Date	Comp. Date	GL Elev. (ft)	TD (ft)	County	Latitude	Longitude	Total Perfs (ft)
1	Ben Hinkle 30-1	15-099-23466	5/17/2004	6/1/2004	840	808	Labette	37.2363692	-95.3589479	17
2	Theodore Housel 28-1	15-125-30553	6/15/2004	6/28/2004	946	1137	Montgomery	37.3230323	-95.5442702	
3	Baugher Trust 1-11	15-099-23519	6/6/2004	6/29/2004	914	836	Labette	37.3600367	-95.2965286	
4	Middleton 9-1	15-133-25986	1/22/2004	1/29/2004	1036	1162	Neosho	37.4551268	-95.4356287	11
5	Nunnenkamp 5-3	15-205-27040	12/13/2006	12/18/2006	821	1193	Wilson	37.5553595	-95.6824155	19
6	Triplett 25-2	15-133-27481	8/19/2008	8/26/2008	982	1105	Neosho	37.4917915	-95.3891812	22
7	RWJ Farms 29-2	15-205-27521	4/18/2008	4/23/2008	932	1296	Wilson	37.5788816	-95.6766792	16
8	Lester Arthur 26-2	15-133-26862	4/11/2007	4/19/2007	1051	1273	Neosho	37.5822550	-95.5230407	24
9	Jerry Brant 3-4	15-133-27339	8/20/2008	8/27/2008	960	1115	Neosho	37.5508170	-95.4229279	
10	William Stich 1-1	15-133-26271	1/19/2005	2/10/2005	958	1014	Neosho	37.5492966	-95.3813417	7
11	Joseph Stich 8-1	15-133-26241	11/22/2004	12/3/2004	966	979	Neosho	37.5346976	-95.3549924	
12	MIH Alexander 18-3	15-133-27276	11/27/2007	12/4/2007	966	997	Neosho	37.6906333	-95.2541504	23
13	King Farms 5-1	15-133-27349	1/4/2008	1/10/2008	904	994	Neosho	37.6360933	-95.3495515	
14	Teleconnect Inc. 23-1	15-133-27092	9/10/2007	9/27/2007	900	913	Neosho	37.5950501	-95.2947392	23
15	Kepley RA 23-1	15-133-26462	1/26/2006	2/9/2006	985	1212	Neosho	37.5966104	-95.5093611	26
16	Cheyney Land 24-4	15-133-27493	8/26/2008	9/2/2008	945	1090	Neosho	37.5886442	-95.3961138	

Appendix A. Basic well information for dataset. Location, well names, and API numbers were supplied by Post Rock Energy. All other information was taken from well log headers.

Appendix B - Gas composition and isotopes data

Sample	He	Ar	O_2	CO_2	N_2	C_1	C_2	C_3	iC_4	nC_4	iC_5	nC_5	C_6+	$\delta^{13}CO_2$	$\delta^{13}C_1$	δDC_1
#	%	%	%	%	%	%	%	%	%	%	%	%	%	‰	‰	‰
1	0.0194	0.0094	0.046	1.07	0.76	98.06	0.0366	0.0011	0.0002	nd	nd	nd	nd	2.70	-62.23	-220.4
2	0.0279	0.0131	0.062	1.53	0.97	96.79	0.266	0.226	0.0252	0.0513	0.0104	0.0100	0.0185	4.27	-60.50	-224.9
3	0.0311	0.0128	0.020	0.47	0.99	98.45	0.0205	0.0023	0.0003	0.0004	nd	nd	0.0004	-5.36	-69.12	-220.7
4	0.0504	0.0300	0.34	0.78	2.54	96.24	0.0210	0.0009	nd	nd	nd	nd	nd	6.67	-57.67	-219.7
5	0.0139	0.0139	0.033	1.05	0.87	97.93	0.0669	0.0156	0.0014	0.0015	0.0002	0.0001	0.0002	4.49	-57.57	-224.1
6	0.101	0.0142	0.037	1.44	1.22	97.14	0.0346	0.0065	0.0006	0.0009	0.0002	0.0002	0.0005	2.87	-62.75	-228.2
7	0.0397	0.0251	0.040	0.58	2.79	96.31	0.0485	0.0428	0.0099	0.0250	0.0105	0.0122	0.0624	5.02	-56.50	-217.2
8	0.0186	0.0080	0.068	1.70	0.62	97.31	0.200	0.0520	0.0075	0.0092	0.0023	0.0017	0.0031	7.60	-61.48	-218.2
9	nd	0.0078	0.051	1.36	0.57	97.98	0.0276	0.0027	0.0009	0.0011	0.0009	nd	0.0005	7.65	-57.26	-224.9
10	nd	0.0113	0.045	1.24	0.66	98.02	0.0222	0.0005	nd	nd	nd	nd	nd	8.04	-57.03	-222.6
11	0.0361	0.0136	0.081	1.47	0.65	97.71	0.0361	0.0008	0.0002	0.0001	nd	nd	nd	5.07	-59.25	-224.9
12	0.0242	0.0167	0.079	1.10	1.92	96.82	0.0318	0.0037	0.0035	0.0008	0.0008	nd	0.0004	9.24	-60.75	-223.2
13	0.0196	0.0264	0.042	0.48	3.97	95.33	0.0581	0.0338	0.0048	0.0083	0.0028	0.0026	0.0172	-1.08	-63.47	-222.4
14	nd	0.0156	0.073	0.49	0.91	98.48	0.0276	0.0003	nd	0.0001	nd	nd	nd	-0.70	-69.95	-220.6
15	0.0124	0.0249	0.042	0.69	2.70	96.51	0.0199	0.0014	0.0001	0.0002	nd	nd	nd	6.40	-59.29	-219.2
16	nd	0.0130	0.048	1.18	0.71	98.02	0.0257	0.0009	nd	0.0001	nd	nd	nd	6.21	-59.46	-223.6

Appendix B. Gas composition and Isotope values for selected Cherokee Basin wells. The result nd means the value was below detection limit.

Appendix C - Water chemistry and isotopes data

Sample #	Temp °C	pH	HCO3 mg/L	Alk mg/L CaCO3	Cl mg/L	SO4 mg/L	Br mg/L	Na mg/L	K mg/L	Mg mg/L	Ca mg/L	Fe mg/L	Percent Balance	TDS	$\delta^{13}CO_2$ ‰	$\delta^{13}C_1$ ‰	δDC_1 ‰	$\delta D\ H_2O$ ‰	$\delta^{18}O\ H_2O$ ‰	Cl/Br
1	18	7.15	346.5	284.3	35710	4.436666667	172	17650	68	1013	1200	83.9	-5.2	56532	2.70	-62.23	-220.4	-37.9	-6.22	207.6
2	18	6.75	440.5	361.3	48790	10.71666667	292	23620	118	1912	1336	30.7	-5.0	76911	4.27	-60.50	-224.9	-35.8	-5.56	167.1
3	18	6.98	234.9	192.7	28840	5.156666667	125	14920	73	785	966	12.2	-3.5	46154	-5.36	-69.12	-220.7	-38.8	-6.32	230.7
4	19	6.73	325.2	266.9	35930	4.976666667	116	17830	152	795	1835	21.4	-4.3	57276	6.67	-57.67	-219.7	-48.7	-7.06	309.7
5	17	6.55	215.4	176.7	58540	0.666666667	268	28050	123	1830	2345	16.5	-5.3	91565	4.49	-57.57	-224.1	-38.0	-5.37	218.4
6	21	6.81	317.3	260.2	29900	4.026666667	103	15560	116	649	1492	6.6	-2.5	48410	2.87	-62.75	-228.2	-50.6	-7.39	290.3
7	25	7.01	240.4	197.2	39890	3.866666667	132	20790	184	675	1591	3.1	-4.0	63707	5.02	-56.50	-217.2	-48.5	-6.83	302.2
8		6.99	304.4	249.7	24310	3.156666667	120	13200	65	501	468	8.4	-3.9	39230	7.60	-61.48	-218.2	-37.4	-5.85	202.6
9	15	6.78	381.3	312.8	44080	5.336666667	174	20860	95	1240	1724	36.5	-6.5	68909	7.65	-57.26	-224.9	-40.1	-5.71	253.3
10			214.8	176.2	37130	5.556666667	143	16960	83	808	1439	n.d.	-9.0	56961	8.04	-57.03	-222.6	-41.6	-6.14	259.7
11	28	6.76	518.3	425.2	21300	5.136666667	72	11900	93	346	707	0.4	-2.2	35367	5.07	-59.25	-224.9	-47.9	-7.18	295.8
12	17	7.54	289.2	237.2	26220	6.856666667	113	13670	80	695	866	1.7	-3.4	42179	9.24	-60.75	-223.2	-38.8	-6.17	232.0
13	18	7.55	214.8	176.2	23440	4.966666667	95	12670	79	486	837	3.3	-2.4	38006	-1.08	-63.47	-222.4	-42.5	-6.42	246.7
14															-0.70	-69.95	-220.6			
15	18	7.39	263	215.5	24240	2.996666667	102	13110	79	523	844	24.4	-2.3	39404	6.40	-59.29	-219.2	-40.5	-6.27	237.6
16	16	7.1	203.2	166.7	35680	4.656666667	151	18260	99	859	1466	62.6	-3.5	56958	6.21	-59.46	-223.6	-39.6	-5.93	236.3

Appendix C. Water chemistry and isotope values for selected Cherokee Basin wells.

Appendix D - Raw culturing results

Sample #	Control 1 (% CH4)	Control 2 (% CH4)	Acetate Culture (% CH4)	Methanol Culture (% CH4)	H_2 Culture (% CH4)
1	0.67	0.87	9.64	6.78	5.52
2	nd	nd	9.16	7.60	7.31
3	nd	nd	1.11	4.88	4.98
4	nd	0.15	2.56	5.98	6.75
5	nd	nd	2.44	6.12	7.08
6	0.16	0.11	2.30	6.87	4.70
7	nd	nd	8.56	6.62	6.88
8	0.14	0.15	2.50	5.23	5.53
9	nd	nd	3.95	6.72	6.99
10					
11	0.11	nd	9.13	6.77	6.95
12	0.49	0.74	2.56	5.82	7.15
13					
14					
15	nd	nd	6.50	7.93	7.16
16	nd	nd	3.46	6.31	3.83

Appendix D. Raw culturing results from selected wells in the Cherokee Basin. Values are percent of CH_4 headspace gas at the end of culturing experiment. Wells without culture data did not have water collected for culturing, or the amount of water available was limited and was used for other analyses.